Chin. J. Astron. Astrophys. Vol. 6 (2006), No. 6, 741–750
(*http://www.chjaa.org*)

Chinese Journal of
Astronomy and
Astrophysics

Formation of the CME Leading Edge Observed in the 2003 February 18 Event *

Xing-Ming Bao[1], Hong-Qi Zhang[1] and Jun Lin[2,3]

[1] National Astronomical Observatories, Chinese Academy of Sciences, Beijing 100012; *xbao@bao.ac.cn*
[2] National Astronomical Observatories / Yunnan Observatory, Chinese Academy of Sciences, Kunming 650011
[3] Harvard-Smithsonian Center for Astrophysics, 60 Garden Street, Cambridge, MA 02138, USA

Received 2006 February 9; accepted 2006 August 27

Abstract This work investigates a typical coronal mass ejection (CME) observed on 2003 February 18, by various space and ground instruments, in white light, Hα, EUV and X-ray. The Hα and EUV images indicate that the CME started with the eruption of a long filament located near the solar northwest limb. The white light coronal images show that the CME initiated with the rarefaction of a region above the solar limb and followed by the formation of a bright arcade at the boundary of the rarefying region at height $0.46\,R_\odot$ above the solar surface. The rarefying process synchronized with the slow rising phase of the eruptive filament, and the CME leading edge was observed to form as the latter started to accelerate. The lower part of the filament brightened in Hα as the filament rose to a certain height and parts of the filament was visible in the GOES X-ray images during the rise. These brightenings imply that the filament may be heated by the magnetic reconnection below the filament in the early stage of the eruption. We suggest that a possible mechanism which leads to the formation of the CME leading edge and cavity is the magnetic reconnection which takes place below the filament after the filament has reached a certain height.

Key words: Sun: coronal mass ejections (CMEs) – Sun: filaments – Sun: flares

1 INTRODUCTION

Coronal Mass Ejections (CMEs) are sudden expansions of magnetic field and plasma from the Sun into interplanetary space. Observations show that fast CMEs are closely related to activities on the solar surface, such as flares and filament eruptions (Munro et al. 1979). The onset of CMEs has been extensively studied for many years since it is closely related to the driving mechanisms of both eruptive prominence and solar flare. Zhang et al. (2001a) showed that the initial phase of CMEs always occurred before the onset of their associated flares. The well-known result that eruptions of filaments begin several minutes before the impulsive phases of flares indicates that the filaments are not driven by flare plasma pressure (Kahler et al. 1988). Since CME initiations are difficult to identify, and since filament eruptions are often observed before the CME, initial filament activities are considered to be a trigger for subsequent CMEs (Neupert et al. 2001). However, the study of a slow CME by Srivastava et al. (2000) suggested that the CME and its associated prominence resulted from a common cause, namely, a global reconstruction of the coronal magnetic field. Many pieces of observational evidence showed that CMEs are not caused by their associated flares (Kahler 1992). Harrison (1995) argued that CMEs and flares are symptoms of the same magnetic "disease" and one does not trigger the other. Instead of being causally related, CMEs, flares and eruptive prominences are thought to be the different manifestations of a single physical process in solar eruptions (Forbes 2000a).

∗ Supported by the National Natural Science Foundation of China.

Because the energy that drives the above eruptive phenomena is stored in the coronal magnetic field, and the latter is anchored with its footpoints in the photosphere and evolves in response to the motion of the photospheric material (e.g., Forbes 2000b; Klimchuk 2001; Priest & Forbes 2002), CME initiation should be closely related to changes in the magnetic field on the solar surface. Zhang et al. (2001b) studied a halo CME that was associated with an eruptive prominence. They found that the apparent change in the magnetic field on the surface is caused by magnetic flux cancellation, and that the eruption take place when the amount of the cancelled magnetic flux exceeds a certain critical value. Lin et al. (2001) pointed out theoretically that the loss of equilibrium in the magnetic field that eventually triggers the eruption usually occurs when about 20% of the original magnetic flux on the surface is cancelled.

New emerging magnetic flux also plays an important role in triggering eruptions. Feynman & Martin (1995) presented observational evidence that eruptions of quiescent prominences and associated CMEs sometimes occur as a consequence of interaction between newly emerging active regions and the pre-existing large-scale magnetic field containing the prominence. After studying three events, Wang & Sheeley (1999) revealed the relationship of the eruption to the newly formed bipolar active regions. Chen & Shibata (2000) and Lin et al. (2001) confirmed theoretically the importance of the new emerging flux in triggering the eruption.

Before observation in space became available, relating solar flare, eruptive prominence and CME to one another was not an easy job because it was difficult to observe CMEs and their source regions simultaneously, for CMEs are best observed over the solar limb while flares and eruptive prominences are best observed on the solar disk. Combining observational data obtained with various instruments both on the ground and in space allow us to investigate various manifestations of a single eruptive process comprehensively. The cool material in the filament seen in absorption is probably the best tracer of the origin and development of CMEs (Maričić et al. 2004). Usually, CMEs are first observed as a bright front in the coronal images at a height around 0.5 $R_\odot$ (Fisher et al. 1981; Gopalswamy et al. 1997; Srivastava et al. 2000), and become fully developed at altitudes of 1 $R_\odot$ above the solar limb.

Formation of the leading edge of the CME is an intriguing problem which has puzzled solar physicists for a long time. Fisher et al. (1981) presented a study of a CME observed in the height range 1.2 to 2.2 $R_\odot$ and found that there is a rarefaction surrounding the erupting prominence before the bright CME loop formed. Dere et al. (1997) studied a CME which was associated with an eruptive prominence commencing with a dark void within a bright loop-like outer shell. The bright arc of CME is thought to result from the pileup of the helmet streamer which overlies the eruptive region (Plunkett et al. 2002). On the basis of the catastrophe model, Lin & Soon (2004) and Lin et al. (2004) studied the evolution of morphological features of CMEs. They suggested that the dense shell at the outer edge surrounding the CME bubble may correspond to the CME's leading edge, the rapid expanding CME bubble constitutes the dark void with a lower density, and the filament (modelled by the flux rope) within the CME bubble is the bright core.

Magnetic reconnection plays an important role in the above processes and in producing various morphological features (Martens & Kuin 1989; Forbes & Priest 1995; Lin & Forbes 2000; Lin 2002). With the system losing its mechanical equilibrium, the flux rope is thrust upward and the closed magnetic field is severely stretched such that it effectively opens up, and a current sheet forms in the wake of the flux rope separating two magnetic fields of opposite polarity. Through magnetic reconnection in the current sheet, the free energy previously stored in the magnetic field is converted into kinetic energy, causing ejection of magnetic flux and plasma that produce CMEs, and thermal energy that heats up the atmosphere, producing flares with separating flare ribbons on the surface and growing flare loops in the corona as the most magnificent features.

With the reconnected magnetic flux being sent towards the solar surface via the lower tip of the current sheet to produce the flare loop system, conservation of magnetic flux outside the diffusion region (or the current sheet) and the property of the magnetic field everywhere being divergence-free require the same amount of the reconnected magnetic flux to be sent upward through the upper tip of the current sheet, creating the fast expanding CME bubble. The plasma associated with the flux fills the outer shell of the ejecta. Lin et al. (2004) and Lin & Soon (2004) tentatively identified the outer shell, the expanded bubble and the flux rope with the leading edge, void and core of the 3-component CME structure (Hundhausen et al. 1994; Low 2001), respectively.

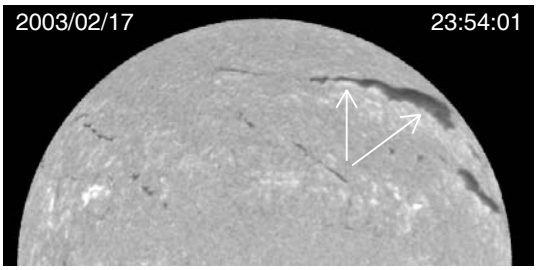

Fig. 1 Hα image 2 hours prior to the eruption taken by PICS of MLSO. Arrows mark the filament that was to erupt.

In this paper, we present an analysis of a typical CME of 3-component structure that occurred on the solar northwest limb and was associated with a polar crown filament eruption and a two-ribbon flare on 2003 February 18. Though the X-ray flux of the flare was weak, relatively slow initiation of this eruption allows us to examine the process in the early phase in detail. The main purpose of this work is to study the formation of various components of the CME and their temporal relation to the eruptive prominence as well as to the flare. Evolution in the morphological features of the eruptive prominence in the early stage observed at various wavelengths is also examined. The observational data studied in this work will be described in the next section. We analyze these data and give our results in Section 3, a discussion is given in Section 4, and finally we summarize the present work in Section 5.

2 OBSERVATIONS

The 2003 February 18 event started with the eruption of a long filament located near the northwest solar limb (N30–43, W40–80). It was observed by several instruments both in space and on the ground, including the Extreme Ultraviolet Imaging Telescope (EIT), the Large Angle and Spectrometric Coronagraph Experiment (LASCO) on board the Solar Heliospheric Observatory (SOHO), the Geostationary Operational Environmental Satellite (GOES), the Polarimeter for Inner Coronal Studies (PICS) and the Mark IV K-coronameter (MK4) at the Mauna Lao Solar Observatory (MLSO). The filament had kept stable for four days before it erupted on February 18. Figures 1 shows the Hα image taken by PICS at MLSO 2 hours prior to the eruption. The arrows indicate the filament before erupted. Most Hα images used in this study were taken by PICS, which is a telescope with a removable occulting disk which allows us to observe the solar limb and the disk alternatively. The field of view (FOV) of PICS ranges from 0 to 2.25 $R_\odot$ and the cadence is 3 minutes. Conjoining the Hα image of the disk and that of the limb makes it possible to capture the early stage of an eruptive prominence from the solar surface to the lower corona [1]. The EIT 195 Å images with cadence of 12 minutes allow us to study the evolution of the erupting filament in the lower corona and the flare ribbons on the disk. The original EIT 195 Å movies are available at the SOHO web site.

The data from the Solar X-ray Imager (SXI) on GOES with cadence of 4 minutes and spatial resolution of 5 arcsec per pixel are also used in this study for investigating the morphological features of the erupting filament and flare ribbons in the temperature range from 10^6 to 10^7 K. Although the images are fuzzy and objects observed clearly at the other wavelengths did not have sharp edges in soft X-ray, blurred outlines of the erupting filament and the associated flare can still be roughly seen from the gif animations [2] by comparing the EIT 195 Å and the Hα movie frames. The MK4 white light images provide us a view of the inner corona from 0.08 to 1.85 $R_\odot$ with cadence of 3 minutes. The FOVs of LASCO C2 and C3 are in the height range of 2–30 $R_\odot$ from the heliospheric center.

Thus, by combining these data, we were able to investigate the take-off and the subsequent development of an eruptive prominence from the solar surface to 6 $R_\odot$ in various wavelengths covering temperatures between 10^4 and 10^7 K. The significance of the present work is that analyzing the multi-wavelength

[1] GIF animation is available at *http://sun.bao.ac.cn/staff/baoxm/halpha_0218.gif*

[2] *http://sun.bao.ac.cn/staff/baoxm/sxi_0218.gif*

data allows us to trace and investigate the formation and evolution of the front edge of a CME with three components.

3 DATA ANALYSES AND RESULTS

The early stage of the eruption is well displayed in Figure 2 which includes the Hα, the EIT 195 Å, and the soft X-ray images of the eruptive prominence. The upper row panels in Figure 2 are composites of the Hα images of the disk and those with the disk blocked, to make clearly visible structures of the filament both inside and outside the solar disk (Fig. 2(a) through 2(d)). At 01:50 UT, the lower part of the filament became bright (indicated by the arrow in Fig. 2(a)) when the filament just lifted to about 9.0×10^4 km. At 01:59 UT the bright feature expanded to the other parts of the filament (indicated by the arrow in Fig. 2(b)) with the filament moving to 1.6×10^5 km. The prominence kept expanding at 02:11 UT (Fig. 2(c)), and its apex became invisible after 02:26 UT (Fig. 2(d)).

The EIT 195 Å and the soft X-ray counterparts of the above Hα images are displayed in Figure 2(e) through 2(h) and Figure 2(i) through 2(l), respectively. Comparing Figures 2(a) and 2(b) with Figures 2(f) and 2(g), we noticed that brightening of the associated flare occurred earlier in Hα than in EUV. With careful studies of the SXI movie, a fuzzy but visible filament profile is recognized as the rising filament, while the filament could hardly be discerned in X-ray before it moved up (comparing Fig. 2(a) and 2(i)). The top of the filament in the SXI image (indicated by the arrow in Fig. 2(j)) appeared unusually bright relative to other part of the filament at 02:01 UT, and two bright points appeared in the footpoints of the filament. The bright point at the top of the filament disappeared immediately while the two bright points in the footpoints got brighter, corresponding to the Hα and EIT 195 Å flare ribbons (Fig. 2(k) and 2(l)). This indicates that the top and the footpoints of the filament were heated to a high temperature of more than 10^6 K.

Considering the associations among solar flares, eruptive prominences and CMEs (e.g. Lin & Forbes 2000; Lin 2004), we understand that such brightenings indicated that heating was taking place with the thermal conduction front and the energetic particles from the magnetic reconnecting site (or the current sheet) behind the CME (or the eruptive prominence) dumping their energy in the lower atmosphere (see also Forbes & Acton 1996). The above phenomenon suggests that the energy from the reconnection region was first dumped in the chromosphere (Hα brightening), then in the high layers (EUV brightening).

In the EIT 195 Å images, the flare developed two separating parallel ribbons and a growing flare loop system (Fig. 2(g) and 2(h)), and some bright features in soft X-ray became visible simultaneously, which were likely to be the top of the eruptive prominence (Fig. 2(j)) and the flare ribbons (Fig. 2(k) and 2(l)). This indicated that the lifted part of the filament was heated to higher temperature. Since the dynamical range of the SXI images is limited, the bright structures of the filament cannot be easily recognized in the lower panels of Figure 2, but they can be seen in the more detailed gif movie mentioned earlier. These bright features correspond to those in the Hα movies. The flare loops appeared clearly in the EIT 195 Å images after 03:30 UT and lasted more than 3 hours as the flare ribbons faded out. At the same time, the flare loops in soft X-ray appeared as blurred bright emission features due to low spatial revolution.

Before the eruptive prominence completely left the FOVs of the PICS and EIT 195 Å images, the disturbance in the corona by the resultant CME could already be recognized in the MK4 white light images (Fig. 3), which show that the disturbance started with rarefaction of a region above the solar limb, its area slightly increasing and its brightness decreasing gradually (Fig. 3(a) through 3(d) and accompanied gif animation[3]). The rarefaction commenced to emerge from the surroundings at 01:52 UT (indicated by the white arrow in Fig. 3(c)). At 01:58 UT the CME leading edge formed on the boundary of the rarefying region (Fig. 3(e)) at altitude 1.46 $R_\odot$ and became more prominent as it reached 1.65 $R_\odot$ at 02:01 UT (Fig. 3(f)). At the same time, the top of the filament just appeared over the limb of the occulting disk. The three-part structure of the CME fully formed at 02:04 UT as shown in Figure 3(g) where EP, CA and LE mark the CME core (or eruptive prominence), cavity and leading edge, respectively. These three components of the CME can be recognized in the LASCO C2 (Fig. 3(h)) and C3 (Fig. 3(i)) images as well. If we time the Hα brightening (Fig. 2(a) and 2(b)) and the formation of the CME leading edge (Fig. 3(c), 3(d), and 3(e)) carefully, we may find that they are correlated to one another pretty well. This confirms indirectly that both

[3] *http://sun.bao.ac.cn/staff/baoxm/mk4_0218.gif*

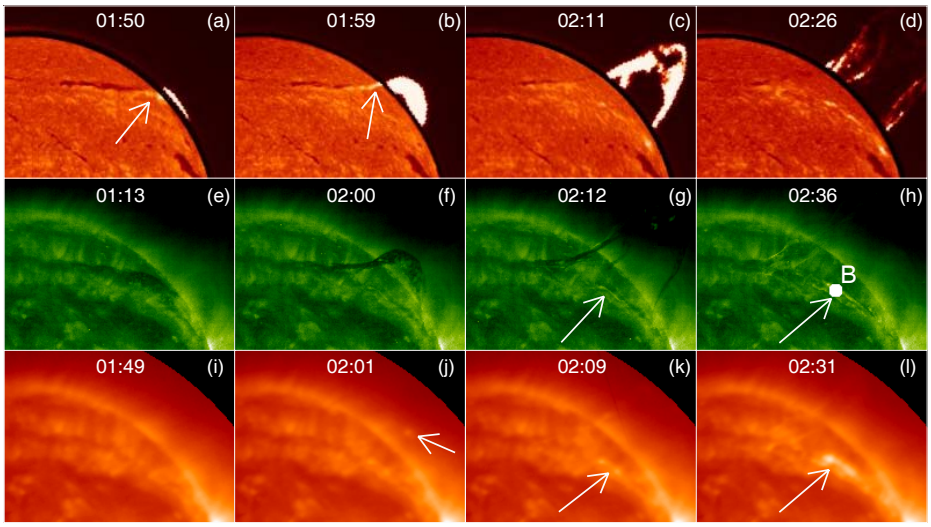

Fig. 2 Evolution of the 2003 February 18 event observed in various wavelengths. Top row panels: Composite of the PICS Hα images of the limb and the disk. The white arrows indicate the emission features appearing in the lower part of the filament. Middle row panels: EIT 195 Å images, the white arrows indicate the flare ribbons. The bright region B in (h) indicates the area where the brightness of EIT 195 Å images plotted in Fig. 5 was measured. Bottom row panels: GOES Soft X-ray Imager (SXI) images, the white arrows indicate the brightenings in the top of the eruptive filament at 02:01 UT and flare ribbons at 02:09 UT and 02:31 UT, respectively.

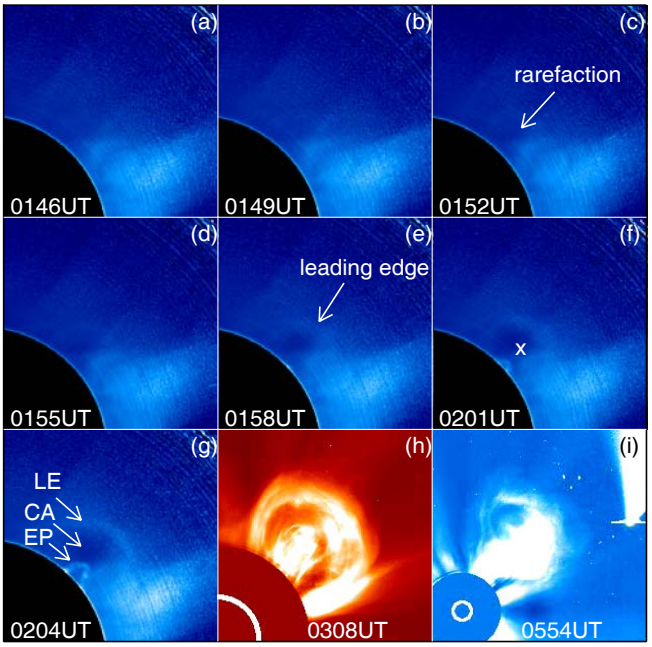

Fig. 3 Evolutions and formations of each component of the CME with typical morphological features. The MK4 images show the formation of the CME leading edge ((a) through (g)). The LASCO C2 and C3 images in (h) and (i) show clear three-component structure. The arrow in (c) indicates where the first rarefaction took place. The arrow in (e) marks the CME leading edge and cavity as well. The cross in (f) indicates the location where the brightness plotted in Fig. 5 was measured. The arrows EP, CA and LE in (g) at 02:04 UT indicate the CME core (filament), cavity and leading edge, respectively.

the CME bubble and the associated flare are products of magnetic reconnection as was predicted by Lin et al. (2004).

Dynamical properties of the eruption may be studied by looking into detailed CME motions. Figure 4 plots the time profiles of various parameters of the CME motions. The initial take-off of each CME component was slow before the CME leading edge formed at 01:58 UT, then apparently sped up (Fig. 4(a) and 4(b)). According to the SOHO LASCO CME Catalog [4], the terminal velocity of the CME was around 1000 km s^{-1}, giving an average acceleration of around 11 m s^{-2} in the height range of 2–30 $R_{\odot}$. Figure 4(b) shows that the main acceleration of each component occurred before they appeared in the FOV of C2, the maximum acceleration could reach up to 1 km s^{-2} (Fig. 4(c)) and quickly decreased as the CME was observed by C2. In this process, the average acceleration is around 135 m s^{-2}.

To show the time sequences of the filament eruption (initiation of the CME) and the associated flare, we plotted the time profiles of the filament height and the CME leading edge height as well as of the GOES X-ray flux in Figure 5(a), and of the brightness of the MK4 and EIT 195 Å images in Figure 5(b), respectively. The brightness of the EIT 195 Å image was measured from points within a circular area (radius five pixels, centered at the bright spot B in Fig. 2(h) on the flare ribbons), and we take the brightness of the flare as the maximum value of the brightness of this area. The brightness of the MK4 image was measured at a fixed point located at about 1.3 $R_{\odot}$ (the cross in Fig. 3(f)). Since the white-light image results from the integrated contribution of the Thomson-scattered photospheric radiation by electrons along the line of sight through the optically thin coronal plasma, the brightness in the MK4 white light images is proportional to the electron density in the corona. The variation of the brightness in corona image is thus a quantitative indicator of change in the coronal material.

Comparing Figures 5(a) and 5(b), we find that the soft X-ray flux increased gradually as the filament rose, and that the associated flare is of class B. Variation of the brightness of the MK4 coronal images, which indicated the initiation of the CME, could be divided into three stages. The first stage is the period from 01:43 UT (the solid vertical line in Fig. 5(b)) to 01:58 UT, when the brightness of the MK4 coronal images start to decrease, gradually, indicating the rarefying process. Usually the brightness decrease is difficult to discern in the MK4 coronal snapshot images. We notice that the rarefying process almost synchronized with the slow-rising phase of the eruptive filament. In the second stage (from 02:01 UT to 02:15 UT), the leading edge of the CME formed and the brightness kept on decreasing to the minimum. The sudden increase in the brightness at the point of measurement (indicated by the arrow filament PT in Fig. 5(b)) is due to the passing of the bright prominence through the point of measurement (the cross in Fig. 3(f)). The third stage is when the brightness began to increase gradually after 02:20 UT. The brightness of the EIT 195 Å images showing the development of the flare ribbons began to increase obviously at 02:12 UT and reached maximum at 02:48 UT. The flare ribbons appeared at 02:12 UT (indicated by the dashed vertical line in Fig. 5(b)) and the filament sped up at around 01:58 UT (Fig. 5(a)) after the CME front commenced to form.

4 DISCUSSION

We presented a study of a typical CME event that took place on 2003 February 28. The CME had an apparent 3-component structure, and the formation of the CME leading edge started with a rarefaction of the region in front of the CME. Since the event occurred near the northwest limb, various manifestations of eruption, such as flare ribbons, CME and filament eruption were well observed. The white-light coronal observations of the early stage evolution of the CME had unprecedentedly high temporal and spatial resolutions and sensitivities. Variations in the brightness of CME images showed how each of the components developed during the eruptive process. This allows us to study the temporal sequences of these various features quantitatively (Figure 5).

Though visible motion of the filament was identified in the EIT 195 Å image between 00:00 UT and 00:12 UT, its slow rise started from 01:30 UT and its rapid acceleration occurred from 02:00 UT. Meanwhile, we notice that the rarefaction of the CME (indicated by the measurable decrease of MK4 brightness) in the period 01:30 UT–02:00 UT almost synchronized with the slow rising of the filament: they were accelerated simultaneously. This indicates that both the CME and the eruptive filament were driven by the same mechanism (Srivastava et al. 2000). Furthermore, we suggest that the initiation of the CME was a gradual

[4] See *http://cdaw.gsfc.nasa.gov/CME_list/*

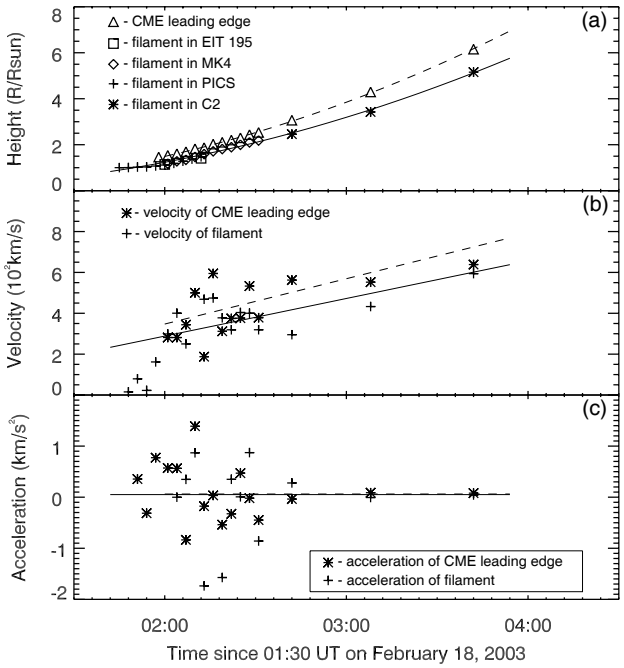

Fig. 4 Height-time (a), velocity-time (b) and acceleration-time (c) profiles of various components of the CME. The dashed (solid) lines indicate quadratic fitting results to the data of the CME leading edge (filament).

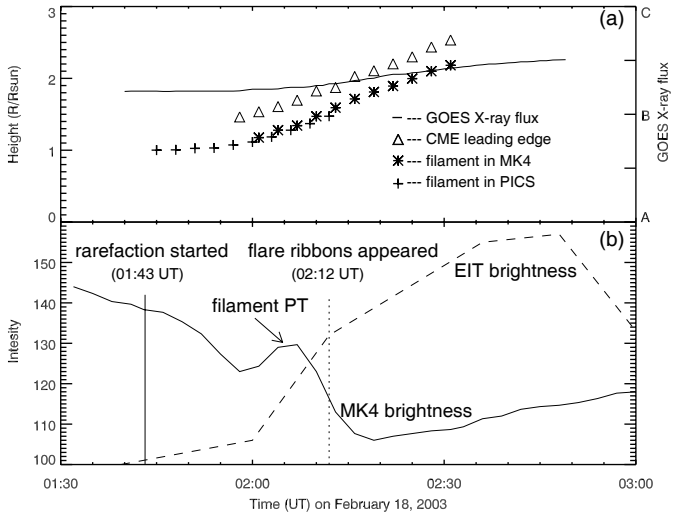

Fig. 5 Time sequences of the filament eruption, flare and CME. (a) Height-time profiles of the CME leading edge and the filament. The GOES X-ray flux is plotted in solid curve. (b) Variations of EIT 195 Å brightness (dashed curve) and of MK4 brightness (solid curve). The solid vertical line indicates the time when the rarefaction above the solar limb started and the dashed vertical line indicates the time when flare ribbons appeared in the EIT 195 Å images. The arrow indicates the increase of brightness during the period when the filament passed through the point marked with a cross in Fig. 3(f).

process, as shown by the slow rising of the filament. Though the X-ray flux was weak (GOES B class), there were clear flare ribbons and loops in the EIT 195 Å images. The flare ribbons were observed at 02:12 UT, some 40 minutes after the start of the CME, and the post-flare loops appeared over the flare ribbons from 03:30 UT. It is notable that even though the flare ribbons looked weak, the final speed of the associated CME reached up to 1000 km s^{-1}. This indicates that fast CMEs may not necessarily be always associated with major flares.

The onset of CME is often a topic of extensive discussion by observers because it is usually difficult to time precisely due to the fact that the inner corona close to the solar limb could hardly be observed by the coronagraph. Previous works estimated CME onset time by extrapolation of the CME altitudes back to the solar surface. This approach obviously suffers from severe uncertainties. Harrison (1995) pointed out that the CME and flare may start at anytime within several tens of minutes of one another. Zhang et al. (2001a) turned to the data from the LASCO C1 to identify the initiation of CME with the moment when the leading edge was first observed. However, many uncertainties remain for the results deduced by this approach because many CMEs (or the associated eruptive prominences) initiate when they are still located on the solar disk. In the present work, on the other hand, we analyzed comprehensively various data obtained by different instruments at different wavelengths, which may reveal a relatively complete scenario of the whole eruptive process. This allows us to determine the CME and the flare onsets without applying extrapolation to our calculations, and to end up with more reliable conclusions.

Results of the present work provide us a method to test the existing models and/or theories of CME and flare, and suggest that many physical and morphological features manifested in the 2003 February 18 event can find their theoretical counterparts in figure 1 of Lin et al. (2004). These features include the slow rising phase of the eruptive prominence, the fast acceleration of the CME, the formation of the CME leading edge, the time the flare at maximum, the CME speed, and so on.

In the very early phase, no brightening appeared at the places where the flare ribbons and loops would be located later, which supports the idea that magnetic reconnection does not occur until the filament reached a certain height. As the filament continued to rise, it stretched the relevant magnetic field lines severely and produced a current sheet separating magnetic field lines of opposite polarities. That rapid accelerations of the filament and the CME leading edge started when the filament became high enough suggests that the system had built up enough kinetic energy when reconnection was initiated in the current sheet (compare the time profiles of the filament heights in Fig. 5(a) with that of the EIT brightness in Fig. 5(b)). Lin et al. (2006) found that the duration of the filament's slow rising phase depends on both the magnetic field and the rate of magnetic reconnection.

With magnetic reconnection occurring in the current sheet, the reconnected plasma and magnetic flux flow out of the current sheet through its upper and the lower tips, respectively. The downward flow (see McKenzie & Hudson 1999; Asai et al. 2004; Sheeley et al. 2004, for observational evidences) eventually reaches the chromosphere, creating bright flare loops and ribbons, and the upward flow (see Ko et al. 2003; Lin et al. 2005, for observational evidence) sweeps the plasma around the flux rope, producing the rarefaction above the filament, and is eventually sealed in the separatrix bubble, fills the outer shell, forming the leading edge of the CME and the rapid expanding CME bubble.

Consulting our observations, we can see that the rarefaction could be discerned in the MK4 images at 01:52 UT, making the start of the upward outflow of the reconnected plasma when the filament had risen to 9.0×10^4 km ($\sim 0.13\,R_\odot$). The CME leading edge formed at 01:58 UT indicates that the outer shell of the flux rope got denser when the filament rose to 1.6×10^5 km ($\sim 0.23\,R_\odot$). Later on, the flare ribbons appeared at 02:12 UT, showing that the chromosphere at the footpoints was heated by the downward outflow and energetic particles accelerated in the current sheet when the filament reached 3.9×10^5 km ($\sim 0.56\,R_\odot$).

In addition to the CME morphological features and their evolutions, another interesting phenomenon during the eruption is also worth mentioning: the appearance of some brightening features in the lower part of the lifted section of the filament during the stage of take-off. The first visible brightenings appeared at 01:50 UT when the eruptive prominence reached about 9.0×10^4 km.

Usually, the filament turns to a prominence with bright emission structure over a dark background when it moves outside of the solar disk . In the present case, however, the brightening features we observed are located in the inner part of the filament when it was still on the solar disk, instead of above the solar limb. Therefore, we rule out the possibility that brightening features in the lower part of the filament are due to

its locating outside of the solar limb. The brightenings in our case should somehow result from heating of the cool filament material.

The mechanism for heating the filament (or prominence) is not very clear, but it may be similar to that for heating the coronal loops. Observations indicate that bright coronal loops exist longer than the cooling time of the plasma in the loop. So, there must be heating process present in the coronal loop in order to balance the cooling. Nano-flare is usually used to explain the heating inside the coronal loops (e.g., Parker 1988; Cargill 1994; Cargill & Klimchuk 1997; Patsourakos & Klimchuk 2005). Parker (1988) used this process to explain the coronal heating, and others (Cargill 1994; Cargill & Klimchuk 1997; Patsourakos & Klimchuk 2005) apply it to heating inside coronal loops. No matter where the process takes place, it assumes that the region where the heating happens is filled with many small elemental threads or strands. These strands are heated randomly by the dissipation of small current sheets that form as a result of interactions among different strands. Parker (1988) argued that the energy deposited in each occurrence of dissipation should be of order 10^{24} erg. The size of energy deposited led to the term "nano-flare".

On the other hand, we also noticed that a fraction of the plasma heated by magnetic reconnection in the current sheet eventually leaves the reconnection site via the upper tip of the current sheet and is sealed in the separatrix bubble. Mixing of this part of plasma with the cold prominence material may heat the latter causing it to change from absorption to emission at various wavelengths. However, this process depends on the complexity of the magnetic structure inside and around the prominence as well as on how the magnetic energy, dissipated by reconnection, is divided between heating and kinetic energy during eruptions.

Overall, heating of prominence in eruption is still the subject of active research, no hard and fast conclusions could yet be drawn. So, more rigorous investigations in both theory and observation are definitely necessary.

5 CONCLUSIONS

The main results of our study are summarized as follows:

(1) The leading edge of the CME formed at the boundary of a rarefying region above the solar limb. The initial front of the CME appeared at height of about $1.46\,R_{\odot}$.
(2) The initiation process of the CME and filament almost synchronized and they are accelerated simultaneously when the CME leading edge began to form. This is consistent with the CME leading edge being a thin shell surrounding the CME bubble and filling with hot plasma.
(3) The CME initiated apparently earlier than the associated flare, as suggested by many observations and theories.
(4) Brightenings in the lower part of the lifted middle section of the filament were observed when the filament reached a certain height. These bright features extended to the two ends of the filament as the filament continued rising. At same time, X-ray bright points appeared at the top and footpoints of the filament. These results suggest that heating inside the filament takes place as a result of magnetic reconnection among the tangling magnetic strands in the filament.

Acknowledgements This work was supported by the National Natural Sciences Foundation of China (NSFC) under Grants 10233050, 10228307, 10611120338 and 10473016, and the National Key Basic Research Program of China under Grants TG 2000078401 and 2006CB806301. JL's work at CfA was supported by NASA under the grant NNG06GI88G to the Smithsonian Astrophysical Observatory. SOHO is a project of international cooperation between ESA and NASA.

References

Asai A., Yokoyama T., Shimojo M. et al., 2004, ApJ, 611, 557
Cargill P. J., 1994, ApJ, 422, 381
Cargill P. J., Klimchuk J. A., 1997, ApJ, 478, 799
Chen P. F., Shibata K., 2000, ApJ, 545, 524
Dere K. P., Brueckner B. E., Howard R. A., et al. 1997, Sol. Phys., 175, 601
Feynman J., Martin S. F., 1995, J. Geophys. Res., 100(A3), 3355
Fisher R., Garcia C. J., Seagraves P., 1981, ApJ, 246, L161

Forbes T. G., Acton L. W., 1996, ApJ, 459, 330
Forbes T. G., Priest E. R., 1995, ApJ, 446, 377
Forbes T. G., 2000a, Philos. Trans. R. Soc. Lond. A., 358, 711
Forbes T. G., 2000b, J. Geophys. Res., 105(A10), 23153
Gopalswamy N., Hanaoka Y., Kundu M. R. et al., 1997, ApJ, 475, 348.
Harrison R. A., 1995, A&A, 304, 585
Hundhausen A. J., Stanger A. L., Serbicki S. A., 1994, in J. J. Hunt, ed., Solar Dynamic Phenomena and Solar Wind Consequences, ESA-SP 373, Noordwijk: ESA, p. 409
Kahler S. W., Moore R. L., Kane S. R. et al., 1988, ApJ, 328, 824
Kahler S. W., 1992, Annu. Rev. A&A, 30, 113
Klimchuk J. A., 2001, In: P. Song, G. Siscoe, H. Singer, ed., Space Weather, AGU Monograph 125, p. 143
Ko Y. -K., Raymond J. C., Lin J. et al., 2003, ApJ, 594, 1068
Lin J., Forbes T. G., Isenberg P. A., 2001, J. Geophys. Res., 106(A11), 25053
Lin J., 2002, Chin. J. Astron. Astrophys. (ChJAA), 2(5), 539
Lin J., 2004, Sol. Phys., 219, 169
Lin J., Forbes, T. G., 2000, J. Geophys. Res., 105(A2), 2375
Lin J., Ko Y.-K., Sui L. et al., 2005, ApJ, 662, 1251
Lin J., Mancuso S., Vourlidas A., 2006, ApJ, 649, 1110
Lin J., Raymond J. C., van Ballegooijen A. A., 2004, ApJ, 602, 422
Lin J., Soon W., 2004, New A., 9, 611
Low B. C., 2001, J. Geophys. Res., 106(A11), 25141
Maričić D., Vršnak B., Stanger A. L. et al., 2004, Sol. Phys., 225, 337
Martens P. C. H., Kuin N. P. M., 1989, Sol. Phys., 122, 263
McKenzie D. E., Hudson H. S., 1999, ApJ, 519, L93
Munro R. H., Gosling J. T., Hildner E. et al., 1979, Sol. Phys., 61, 201
Neupert W. M., Thompson B. J., Gurman J. B. et al., 2001, J. Geophys. Res, 106(A11), 25215
Parker E. N., 1988, ApJ, 330, 474
Patsourakos S., Klimchuk J. A., 2005, ApJ, 628, 1023
Plunkett S. P., Michels D. J., Howard R. A. et al., 2002, Adv. Space Res., 29, 1473
Priest E. R., Forbes T. G., 2002, A&A Rev., 10, 313
Sheeley Jr. N. R., Warren H. P., Wang Y.-M., 2004, ApJ, 616, 1224
Srivastava N., Schwenn R., Inhester B. et al., 2000, ApJ, 534, 468
Wang Y., Sheeley Jr. N. R., 1999, ApJ, 510, L157
Zhang J., Dere K. P., Howard R. A. et al., 2001a, ApJ, 559, 452
Zhang J., Wang J., Nitta N., 2001b, Chin. J. Astron. Astrophys. (ChJAA), 1, 85